IOPscience iopscience.iop.org

Home Search Collections Journals About Contact us My IOPscience

The micropatterning of layers of colloidal quantum dots with inorganic ligands using selective wet etching

This content has been downloaded from IOPscience. Please scroll down to see the full text.

2014 Nanotechnology 25 175302

(http://iopscience.iop.org/0957-4484/25/17/175302)

View the table of contents for this issue, or go to the journal homepage for more

Download details:

IP Address: 157.193.173.166
This content was downloaded on 23/04/2014 at 17:09

Please note that terms and conditions apply.

IOP Publishing Nanotechnology
Nanotechnology **25** (2014) 175302 (11pp) doi:10.1088/0957-4484/25/17/175302

The micropatterning of layers of colloidal quantum dots with inorganic ligands using selective wet etching

Chen Hu[1,2,3], Tangi Aubert[1,3], Yolanda Justo[1,3], Stijn Flamee[1,3], Marco Cirillo[1,3], Alban Gassenq[2,3], Oksana Drobchak[3,4], Filip Beunis[3,4], Günther Roelkens[2,3] and Zeger Hens[1,3]

[1] Physics and Chemistry of Nanostructures Group, Ghent University, Krijgslaan 281-S3, B-9000 Gent, Belgium
[2] Photonics Research Group, INTEC Department, Ghent University-IMEC, Sint-Pietersnieuwstraat 41, B-9000 Ghent, Belgium
[3] Center for Nano- and Biophotonics (NB-Photonics), Ghent University, Belgium
[4] Liquid Crystals and Photonics Group, Ghent University, Sint-Pietersnieuwstraat 41, B-9000 Ghent, Belgium

E-mail: Zeger.Hens@UGent.be

Received 2 December 2013, revised 16 January 2014
Accepted for publication 4 February 2014
Published 10 April 2014

Abstract
The micropatterning of layers of colloidal quantum dots (QDs) stabilized by inorganic ligands is demonstrated using PbS core and CdSe/CdS core/shell QDs. A layer-by-layer approach is used to assemble the QD films, where each cycle involves the deposition of a QD layer by dip-coating, and the replacement of the native organic ligands by inorganic moieties, such as OH^- and S^{2-}, followed by a thorough cleaning of the resulting film. This results in a smooth and crack-free QD film on which a photoresist can be spun. The micropatterns are defined by a positive photoresist, followed by the removal of uncovered QDs by selective wet etching with an HCl/H_3PO_4 mixture. The resulting patterns can have submicron feature dimensions, limited by the resolution of the lithographic process, and can be formed on planar and 3D substrates. It is shown that the photolithography and wet etching steps have little effect on the photoluminescence quantum yield of CdSe/CdS QDs. Compared with the unpatterned CdSe/CdS QD film, only a 10% degradation in the quantum yield is observed. These results demonstrate the feasibility of the proposed micropatterning method to implement the large-scale device integration of colloidal quantum dots.

Keywords: nanocrystals, layer-by-layer deposition, micropatterning, optical lithography, integrated photonics

(Some figures may appear in colour only in the online journal)

1. Introduction

Colloidal quantum dots (QDs) are new optoelectronic materials that raise great interest in the photonics community. Various applications, such as solar cells [1–3], photodetectors [4–6] and light emitting diodes (LEDs) [7, 8], have been demonstrated using different semiconductor QD materials. Hot injection chemical synthesis allows for a low-cost,

 © 2014 IOP Publishing Ltd Printed in the UK

precise and versatile production [9, 10]. In addition, by varying their size, the QD electrical and optical properties (absorption cut-off wavelength, luminescence wavelength) can be easily tuned through the quantum size effect [11]. Furthermore, the fact that these QDs are available in solution allows for large-area heterogeneous integration on substrates by solution-based processes, such as spin casting [12], inkjet printing [13–15], evaporation-controlled self-assembly [16], and Langmuir–Blodgett (LB) [17] or Langmuir–Schaeffer deposition [18, 19]. This offers a considerable cost reduction as compared to thermally evaporated or epitaxially grown layer stacks.

As a new optoelectronic material, one of the applications of colloidal QDs that stands out is the use of QD films as a medium for light absorption and charge carrier transport in photovoltaic energy conversion [20, 21], photodetection [22, 23] and electronics [24, 25]. For example, colloidal quantum dot solar cells with a certified efficiency of up to 7% were recently reported [26], while a hybrid phototransistor consisting of a combination of colloidal quantum dots with graphene was shown to achieve an ultrahigh gain of up to 10^8 electrons per photon [27]. A crucial step for these applications is the replacement of the long, electrically insulating organic ligands that cap as-synthesized QDs by much shorter moieties to enhance the mobility of charge carriers in QD films. While initial procedures involved the exchange of the original ligands for short, bifunctional organic molecules such as hydrazine or dietheylamine, more recent approaches have made use of the replacement of long organic ligands by short, inorganic species such as $Sn_2S_6^-$ or Cl^-. Very often, layers of QDs with short ligands are formed using a layer-by-layer deposition approach, involving the repeated deposition of a layer of QDs stabilized by their long, as-synthesized ligands, followed each time by a ligand exchange step [28–30]. Importantly, this approach does not require a stable dispersion of QDs with short ligands and it enables cracks formed in the layer due to the ligand exchange to be filled in the next deposition step. High electron mobility exceeding 15 $cm^2/(V{\cdot}s)$ was reported recently by Liu *et al* [31] for III-V nanocrystals capped with molecular metal chalcogenide ligands.

Especially in the case of photodetectors or transistors, the suitability of colloidal QDs for solution-based processing offers the possibility of combining QD-based devices with integrated electronic or photonic circuits. This, however, requires the formation of well-defined and aligned patterns of colloidal QD layers. In the literature, different micropatterning processes have been explored, each having their own specific benefits and disadvantages. Lambert *et al* proposed to use Langmuir–Blodgett layer deposition on a silicon substrate that is covered by a patterned resist, which results in a monolayer pattern with micrometer resolution after lift-off [32]. High-resolution nanoscale patterning of QD films was also demonstrated through electron beam (e-beam) lithography [33, 34]. Nevertheless, the long writing time and the high cost of the electron beam lithography makes it less attractive for mass production. A high-throughput micropatterning method with sub-micrometer-scale resolution was realized by a contact printing process [35, 36]. With a key-lock system, a nanoscale patterned QD film can be implemented by e-beam lithography and highly discriminatory binding in a DNA-mediated approach [37, 38]. However, the deposition on a three-dimensional surface such as a photonic integrated circuit and the formation of micropatterned multiple layer QD films still remains challenging. Moreover, none of these approaches can be directly applied for the patterning of QD films with the inorganic ligands that are typically used as the absorber layer in photovoltaic cells and photodetectors or as conductive channel in field effect transistors.

In this study, we use PbS colloidal QDs to demonstrate a novel technique to pattern films of QDs stabilized by inorganic ligands. The PbS QD films are defined using a layer-by-layer approach where each cycle involves the deposition of a QD layer by dipcoating, the replacement of the native organic ligands by metal-free inorganic ligands, such as OH^- and S^{2-} [39], followed by a thorough cleaning of the resulting film. This results in smooth and crack-free QD films. The micropatterns are defined by a positive photoresist, followed by the removal of uncovered QDs by wet etching using an HCl/H_3PO_4 mixture. The resulting patterns can have feature dimensions down to 500 nm, limited by the resolution of the lithographic process, and it is shown that the process applies to 3D substrates as well. To further evaluate the influence of this patterning technique on the properties of the colloidal QDs, films of highly luminescent CdSe/CdS core/shell are treated and micropatterned with the same technique. Photoluminescence analyses demonstrate that more than 90% of the quantum yield remains after photolithography and wet etching. This indicates that the proposed approach allows for the effective micropatterning of QD films without affecting the QD properties.

2. Experimental details

2.1. Materials

Technical oleic acid (OlAc, 90%) was ordered from Sigma-Aldrich. $PbCl_2$ (99.999%), selenium powder (200 mesh, 99.999%), sulfur (99.999%) and trioctylphosphine oxide (TOPO, 98%) were purchased from Alfa-Aesar. CdO (99.999%), and tri-n-octylphosphine (TOP, 97%) was purchased from Strem Chemicals. Technical oleylamine (OlAm, 80–90%) was ordered from Acros. AZ® 5214E image reversal resist for high resolutions was purchased from Microchemicals GmbH. Hydrochloric acid (HCl, 37%) was purchased from VWR. Ortho-phosphoric acid (H_3PO_4, 85%) was purchased from Merck KGaA.

2.2. Synthesis of colloidal quantum dots

The synthesis of OlAm-teminated PbS QDs was based on the method developed by Cademartiri *et al* [40] and described in detail in [11]. A stock solution was prepared by heating a mixture of 0.16 g (5 mmol) S in 15 mL of OlAm under nitrogen for 30 min at 120 °C. In the first step of the synthesis, a mixture of 0.834 g (3 mmol) of $PbCl_2$ and 7.5 mL of OlAm in a three-neck flask was degassed under nitrogen for 30 min at 125 °C. After that, the mixed $PbCl_2$ solution was heated up

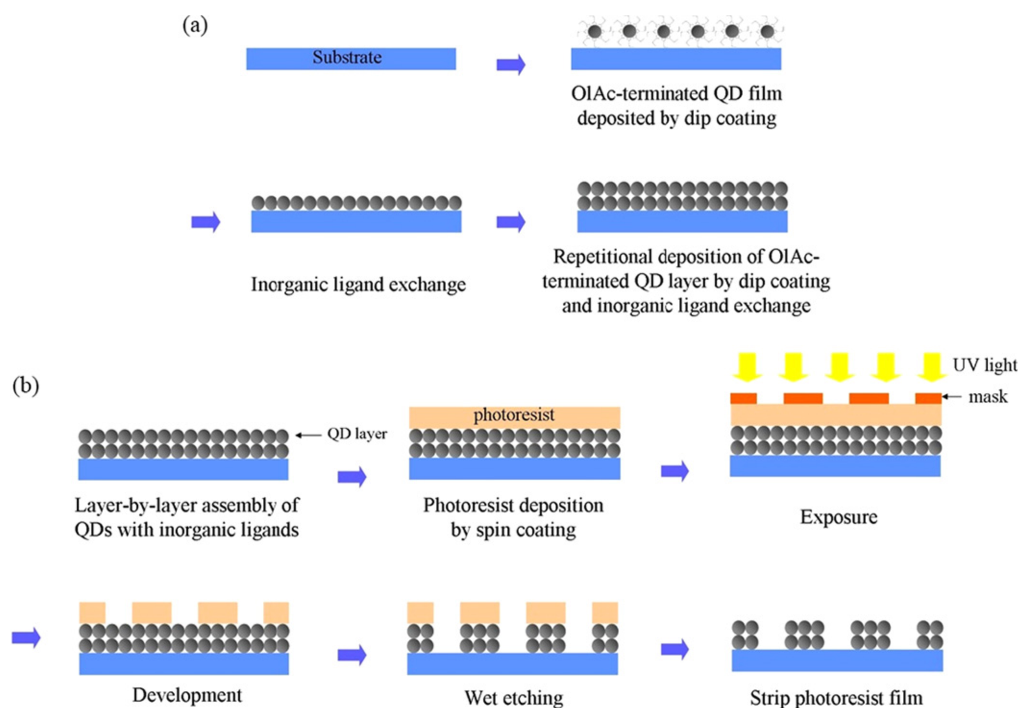

Figure 1. (a) Illustration of the layer-by-layer deposition of the QD film. (b) Process flow of the QD film micropatterning.

to reach the required injection temperature, and then a mixture of 2.25 mL of the OlAm-S stock solution (0.75 mmol of S) and 170 μL (375 μmol, half of the amount of S) of TOP were injected into the flask. After injection, the temperature dropped by ≈5–10 °C, and the resultant growth temperature was maintained through the whole reaction. After the designed growth time, the reaction was quenched by adding a mixture of 10 mL of toluene and 15 mL of MeOH. The resulting synthesis suspension was centrifuged and the supernatant was removed by decantation, after which the PbS QDs were resuspended in 10 mL of toluene. For the PbS QDs studied in this paper, the growth temperature was 160 °C and the growth time was 2 h 30 min. After synthesis, the OlAm ligands were replaced by oleic acid (OlAc) to obtain a ligand shell that can stand successive purification cycles. The ligand exchange was realized by adding OlAc to a toluene suspension of PbS QDs in a volume ratio of 1.5:10 OlAc/toluene. Afterwards, the suspension was purified using methanol (MeOH) and toluene as the non-solvent and the solvent, respectively. Typically, the ligand exchange was repeated twice. After a final precipitation with MeOH, the PbS QDs were resuspended in toluene. The concentration of the resulting QD suspension was determined from the QD absorbance spectrum through the molar extinction coefficient at 400 nm ($\in_{400}$) [11].

The CdSe/CdS core/shell QD synthesis was accomplished by adapting the CdSe/CdS dot-in-rod synthesis procedure developed by Carbone *et al* [41]. CdO (0.25 g), TOPO (3 g) and OlAc (2.35 g) were added to a three-neck flask, and the resulting mixture was flushed with nitrogen and heated at 120 °C for 1 h. The temperature was then increased to 330 °C and 1.8 mL of TOP was injected when the mixture solution became colorless. After the temperature recovered to 330 °C, a mixture of CdSe core QDs (86 mmol) and sulfur (0.12 g) in 1.8 mL of TOP was injected into the flask. The reaction was quenched after 3 min by a sudden drop in the temperature using a water bath, followed by the injection of 10 mL of toluene. Then the QDs were precipitated with isopropanol and MeOH, and were centrifuged. After the supernatant was decanted, the QDs were resuspended in toluene. The precipitation and resuspension were repeated three more times and the CdSe/CdS core/shell QDs were finally resuspended in toluene.

2.3. Fabrication of QD films

In this study, QD films were prepared with a layer-by-layer approach. The corresponding process flow is shown in figure 1(a). Each cycle involves the deposition of a QD layer by dipcoating, the replacement of the native organic ligands by metal-free inorganic ligands, followed by a thorough cleaning of the resulting film. The dipping procedure with ligand exchange can be done repetitively to implement a multi-layer film. Here, PbS QD thin films were formed on Si substrates. CdSe/CdS QD films were formed on cover glass substrates. A layer-by-layer approach was used by dipping the substrate into a PbS or a CdSe/CdS QD dispersion in toluene with a QD concentration in the range of 0.75 to 1 μM and pulling it out at a speed of 80 mm min^{-1}. Before layer-by-layer deposition of the QD films, the Si substrates were treated with HF solution (~10%) for 1 min to remove the native oxide and enhance the hydrophobicity of the surface. After complete drying, the QD film was re-immersed into a solution of either $Na_2S \cdot 9H_2O$ (10 mg mL^{-1}) or KOH (0.01 mg mL^{-1}) in formamide to exchange the OlAc ligands by S^{2-} and OH^- moieties, respectively. After the desired ligand exchange time (typically 60 s for S^{2-} and 10 s for OH^-), the

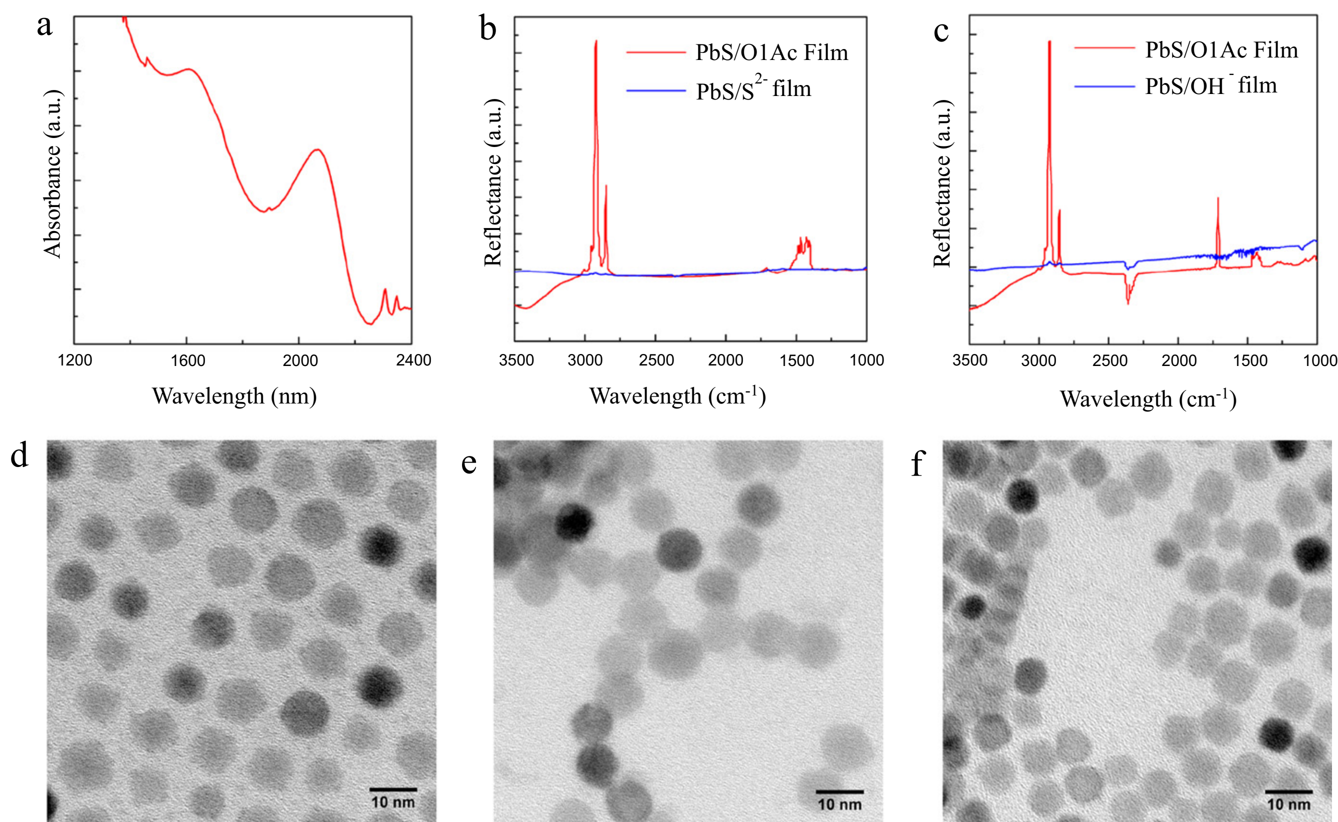

Figure 2. (a) Absorbance spectrum of the PbS QDs used (solvent: tetrachloroethylene). (b) Reflection– Fourier Transform InfraRed (FTIR) spectra of an OlAc-terminated PbS colloidal QD film and a S^{2-}-terminated PbS colloidal QD film after $Na_2S \cdot 9H_2O$ treatment. (c) Reflection–FTIR spectra of OlAc-terminated PbS colloidal QD film and OH^--terminated PbS colloidal QD film after KOH treatment. TEM images of (d) OlAc, (e) S^{2-} and (f) OH^- -terminated colloidal PbS QDs.

sample was washed by immersing it twice in formamide and twice in acetone, followed by a final dip in isopropanol to remove residual impurities induced by the ligand exchange (see supporting information I for details on the cleaning procedure, available at stacks.iop.org/NANO/25/175302/mmedia). Afterwards, the sample was dried under nitrogen. Depending on the experiment, the QD films used in this paper were prepared by repeating the layer-by-layer deposition four to six times. The resulting PbS QD films exhibit a remarkable improvement of photoconductivity compared with OlAc-teminated PbS colloidal QD films as reported in [42], which illustrates that this novel technique is promising for integrated photodetector and photovoltaic applications.

2.4. Photolithography and wet etching

The process flow of the patterning of a QD film formed by the layer-by-layer approach is shown in figure 1(b). In the first step, an AZ® 5214E image reversal resist was spun on top of the QD film by spin coating, and was prebaked for 3 mins at 100 °C to form a robust photoresist layer. Following light exposure and development using a SUSS MA6 mask aligner, a pattern was transferred from a mask to the photoresist layer. Afterwards, an HCl/H_3PO_4 mixture, prepared by mixing 37% HCl and 85% H_3PO_4 solutions, was used as etchant to remove the uncovered parts of the QD film. The volume ratio between the HCl and H_3PO_4 solution in the etchant was ≈1:10. The QD film, covered with patterned photoresist, was immersed into the HCl/H_3PO_4 mixed etchant for the desired etching time to remove the uncovered QDs. In the end, the remaining photoresist layer was stripped from the QD film using acetone, and the sample was cleaned with isopropanol to obtain a micropatterned QD film.

2.5. Characterization of quantum dots and quantum dot films

The absorbance of the colloidal solutions and thin films was evaluated by UV–vis–NIR spectrophotometry (Perkin Elmer Lambda 950). Ligand exchange was analyzed at the level of individual QDs by transmission electron microscopy (TEM, Jeol, FE2200). Samples for TEM were prepared by transferring the QD film to a copper grid with carbon film through dipping. For the ligand exchange sample, the TEM grid with QDs on top was dipped into the ligand exchange solution, followed by a thorough cleaning to get rid of impurities. A Fourier transform infrared spectrometer (FTIR spectrometer, Nicolet 6700) was used to analyse residual organic species in the QD film. The overall morphology of the films was analyzed by means of atomic force microscopy (AFM) measurements (Picoplus, Molecular Imaging) and scanning electron microscopy (SEM, FEI Nova 600 Nanolab Dual-Beam FIB). The film thickness was also derived from AFM

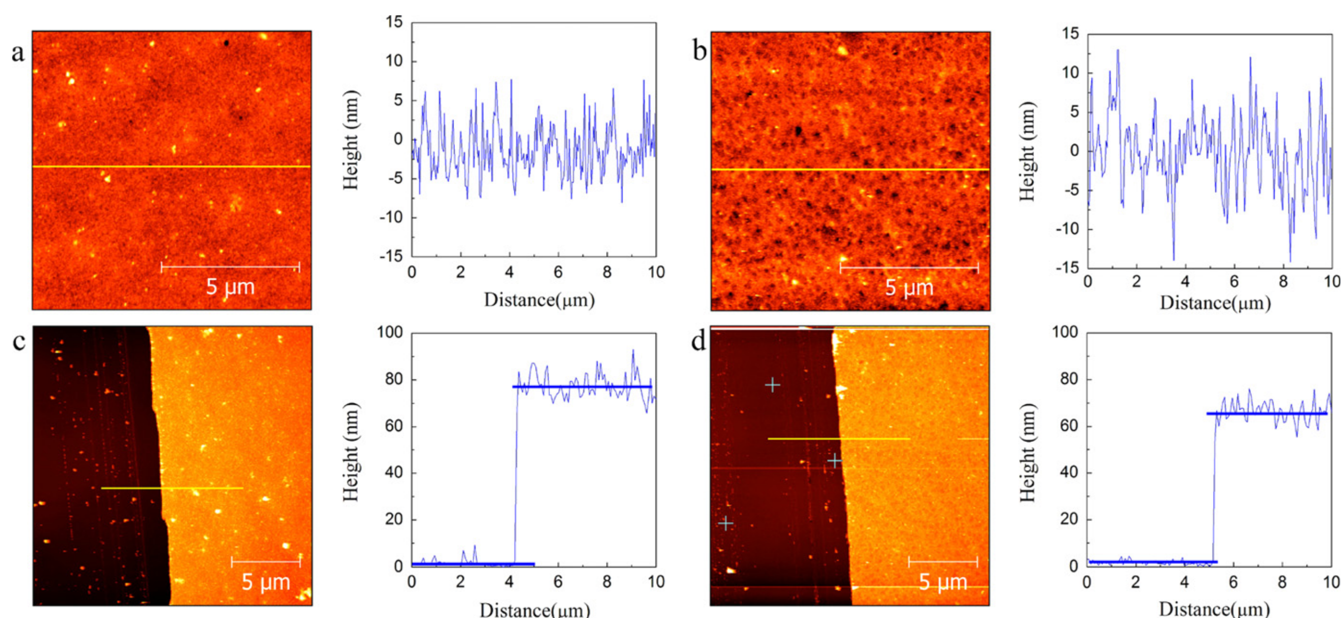

Figure 3. AFM images obtained on (a) PbS/S^{2-} and (b) PbS/OH^{-} QD films prepared by six times layer-by-layer deposition before lithography and micropatterning. The film thickness is determined by the topographic analysis of a deliberately scratched film, both for (c) PbS/S^{2-} and (d) PbS/OH^{-} films. The yellow lines mark the respective cross sections shown.

by measuring the average height profile of a scratch over the entire substrate surface. Photoluminescence measurements were made using an Edinburgh Instruments FLSP920 UV–vis–NIR spectrofluorimeter, using a 450 W xenon lamp as the steady state excitation source and a Hamamatsu R928P PMT detector, which has a response curve between 200 and 900 nm. All measurements were performed for an excitation wavelength of 365 nm and were corrected for the sensitivity of the detector. The quantum yield (QY) of the QDs dispersed in toluene was determined for an excitation wavelength of 365 nm and by comparison with coumarin 2, which has a known PLQY of 92% in ethanol [43]. The QY of the QD films was measured using an integrating sphere (see supporting information II for details, available at stacks.iop.org/NANO/25/175302/mmedia). Fluorescence microscopy (Nikon Eclipse Ti inverted microscope) was used to get the photoluminescence mapping of the micro-patterned film.

3. Results and discussion

3.1. Layer-by-layer assembly of quantum dots with inorganic ligands

In this study, we used colloidal PbS core QDs with a band gap absorbance at 2.2 μm, which corresponds, according to the PbS sizing curve, to a diameter of 9.4 nm [9]. The corresponding absorbance spectrum of these PbS QDs in tetrachloroethylene (C_2Cl_4) is presented in figure 2(a). In order to explore the ligand exchange upon exposure to $Na_2S \cdot 9H_2O$ or KOH solutions, a reflection-FTIR spectrometer was used to analyse organic residues in the QD film. Figure 2(b) shows the reflection-FTIR spectra of a film of OlAc-terminated PbS QDs and of the corresponding QD film after exposure to $Na_2S \cdot 9H_2O$. The characteristic peaks corresponding to C=C stretching around 3010 cm^{-1}, -CH_2 asymmetric stretching around 2920 cm^{-1} and –CH_3 symmetric stretching around 2850 cm^{-1} are almost completely eliminated after ligand exchange, which indicates that most of the OlAc ligands were removed from the QD film. Similar results can we seen in figure 2(c), which shows spectra obtained before and after a KOH treatment. The ligand exchange on a small scale is examined by TEM. The micrographs clearly show that the distance between the PbS QDs—originally dictated by the long chain oleate ligands (figure 2(d))—decreases after $Na_2S \cdot 9H_2O$ (figure 2(e)) or KOH (figure 2(f)) treatments, which is promising to form a close-packed QD film for device applications. Moreover, it appears that the S^{2-} terminated QDs tend to aggregate, opposite from the OH^{-} terminated QDs. We found that if the QD film was too thick before ligand exchange, i.e., when multiple layers were deposited after dip coating, the top few layers of the QD may detach from the film during the ligand exchange. Nevertheless, this can be compensated for by multiple depositions through the layer-by-layer approach.

Figures 3(a) and (b) show AFM images of films made using six deposition cycles of PbS/S^{2-} and PbS/OH^{-} QDs, each involving dipping the substrate into a 0.75 μM PbS QD suspensions in toluene and pulling it out at a speed of 80 mm min^{-1}. Corresponding SEM images are shown in the supporting information (see supporting information III, figure S3, available at stacks.iop.org/NANO/25/175302/mmedia). It follows that the process leads in both cases to the formation of homogeneous and crack-free films over large areas. The RMS roughness as determined from the AFM image amounts to 5.5 nm and 6 nm for PbS/S^{2-} and PbS/OH^{-} films, respectively, a number smaller than the diameter of a single nanocrystal. Before photolithography and micropatterning, a layer

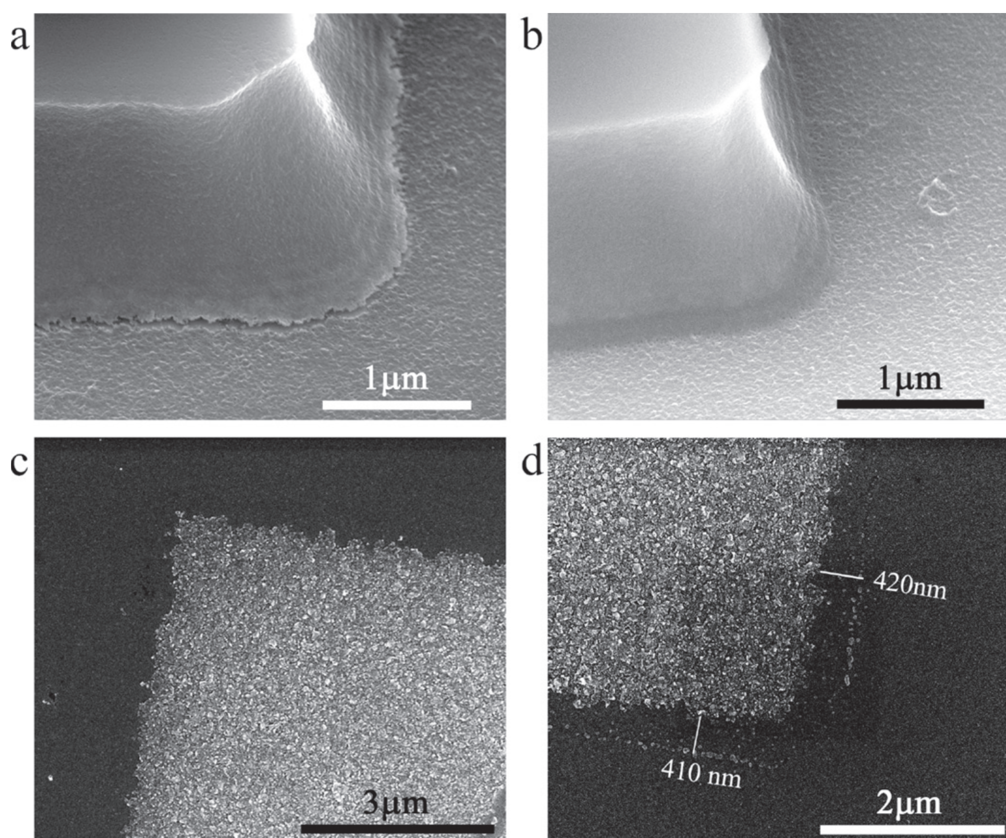

Figure 4. SEM images of a 30 s etching of a micro-patterned S^{2-} terminated PbS QD film with a photoresist formed by etching with a mixture of (a) $1HCl:8H_3PO_4$ or (b) $1HCl:10H_3PO_4$. SEM images of (c) 30 s and (d) 60 s of etching with $1HCl:10H_3PO_4$ of a S^{2-} terminated PbS QD film.

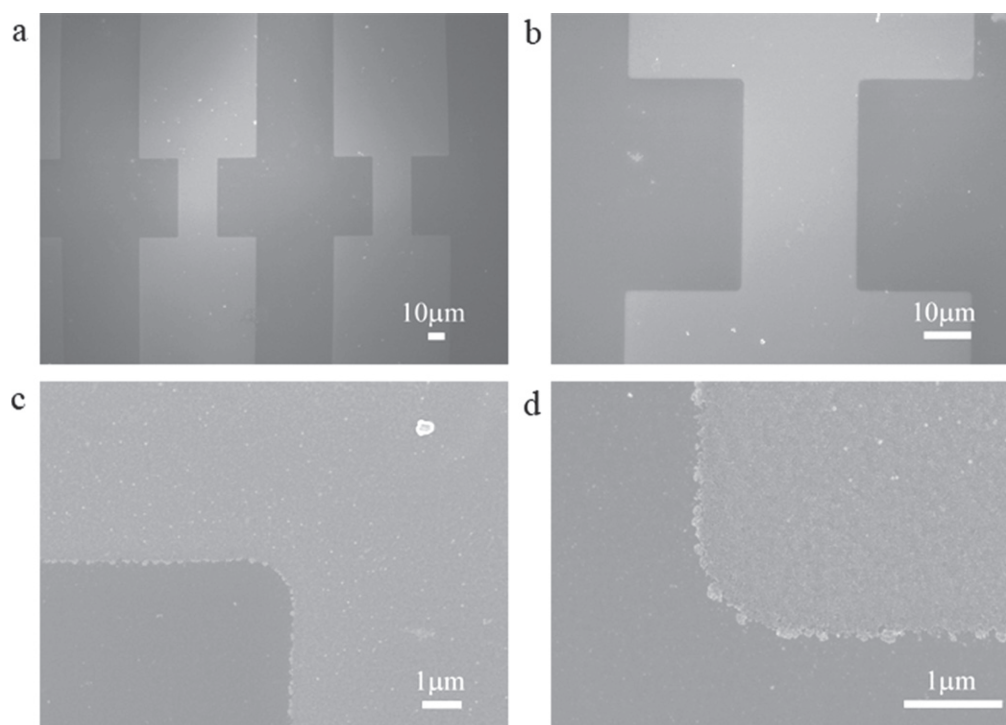

Figure 5. SEM images of the 1 min 40 s' etching of a micro-patterned OH^- terminated PbS QD film by etching with a mixture of $1HCl:10H_3PO_4$, at different magnification scales.

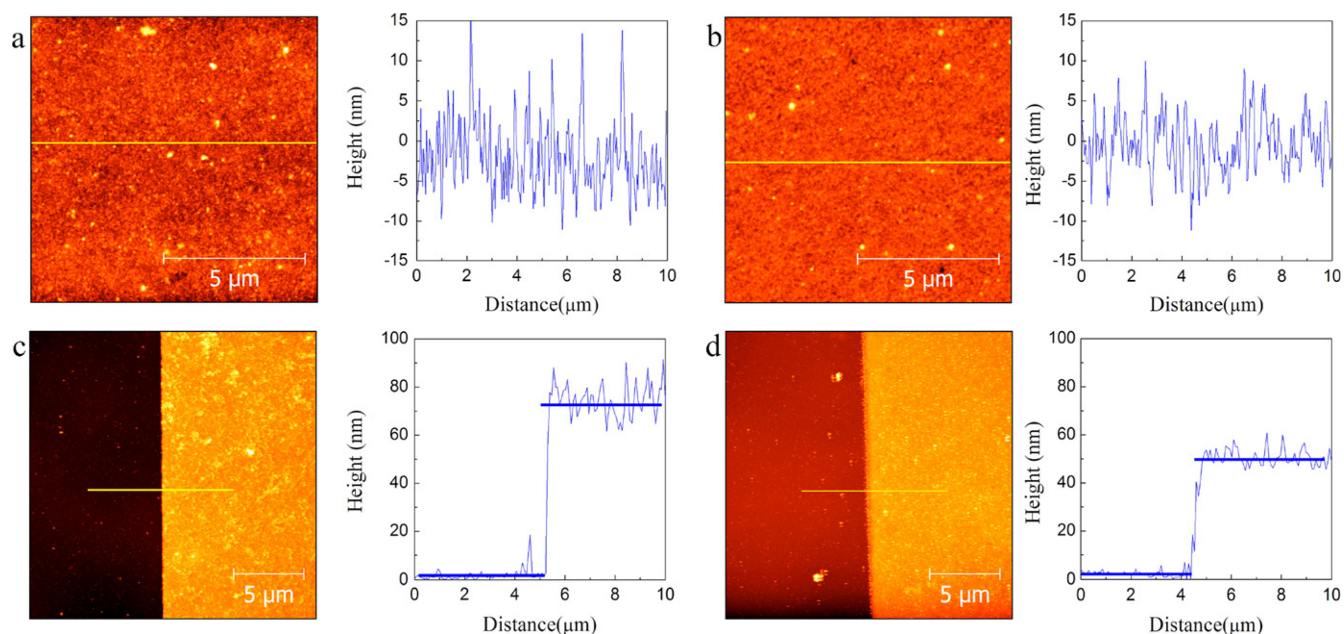

Figure 6. AFM images obtained of (a) PbS/S^{2-} and (b) PbS/ OH^- QD films after micropatterning. The layer thickness is determined by imaging the edge of the QD film, both for (c) PbS/S^{2-} and (d) PbS/OH^- QD films. The films were prepared by six layer-by-layer deposition cycles. The yellow lines mark the respective cross sections shown.

thickness of ≈75 nm and ≈65 nm is found for S^{2-} and OH^- terminated QD films (see figures 3(c) and (d)), respectively, indicating that about one QD monolayer is deposited in each cycle. We thus conclude that the process developed results in smooth and homogeneous films that are well-suited for testing the subsequent processing steps.

3.2. Micro-patterned QD films—2D substrates

To put the proposed micropatterning scheme into practice, a first set of films of PbS QDs films was formed by layer-by-layer deposition using four deposition cycles, each involving dipping the substrate into a 1 μM PbS QD suspensions in toluene and pulling it out at a speed of 80 mm min^{-1}. To optimize the etching step, etching solutions with different HCl/H_3PO_4 ratios were investigated and the etching time was varied. Figures 4(a) and (b) shows SEM images of the micro-patterned PbS/S^{2-} QD films with photoresist on top after a 30 s wet etch using HCl and H_3PO_4 mixing ratios of 1:8 and 1:10, respectively. The gap slit under the photoresist visible when the higher HCl ratio is used (figure 4(a)) indicates that under-etching occurs under these conditions, which is prevented by lowering the HCl concentration (figure 4(b)). Possibly, this is due to the lower viscosity and the concomitantly higher etching speed of etching solutions with a higher HCl content. SEM images of the micro-patterned PbS/S^{2-} QD films after lift-off for different etching times are displayed in figures 4(c) and (d). One can see that after ≈30 s of wet etching (figure 4(c)), the uncovered QD film was almost fully removed from the substrate and a well-defined patterned QD film was obtained. As shown in figure 4(d), increasing the etching time to ≈60 s only promotes under-etching, resulting in the disappearance of the outermost parts of the QD film covered by the photoresist over a depth of 410–420 nm. As a result, we kept the HCl:H_3PO_4 volume ratio for further studies fixed at 1:10 and limited the etching time—depending on the layer thickness—to the lowest time needed to remove all uncovered QDs.

Figure 5 shows SEM images at different magnifications of the micropatterned OH^- terminated PbS QD films formed with the optimized process (etching solution: 1:10 HCl:H_3PO_4; etching time: 100 s and 150 s for PbS/OH^- and PbS/S^{2-}, respectively). For comparison with untreated films, they were again formed using six layer-by-layer deposition cycles in total, dipping the substrate into a 0.75 μM PbS QD suspension in toluene and pulling it out at a speed of 80 mm min^{-1}. As shown in the figure, after stripping the photoresist film, a well-defined QD film is obtained. The resolution of the micropatterning is mainly limited by the optical lithography process, which is ≈0.5 μm. As shown in the supporting information (supporting information IV, figure S4, available at stacks.iop.org/NANO/25/175302/mmedia), similar results are obtained using S^{2-} terminated PbS QD films. An AFM analysis of similar micropatterned films yields an RMS roughness of ≈5.5 nm and ≈4.5 nm for S^{2-} and OH^- terminated PbS QD films, respectively (see figures 6(a) and (b)). Moreover, the layer thickness—in this case simply measured by imaging the transition between the uncovered substrate and the remaining PbS film—for both films amounts to ≈70 nm and ≈50 nm. Hence, only in the case of PbS/OH^-, a somewhat thinner layer is obtained. Therefore, we conclude that the proposed micropatterning process leads to well-defined patterns of PbS QD films with a resolution determined by that of the lithographical process used and without affecting the original morphology of the films.

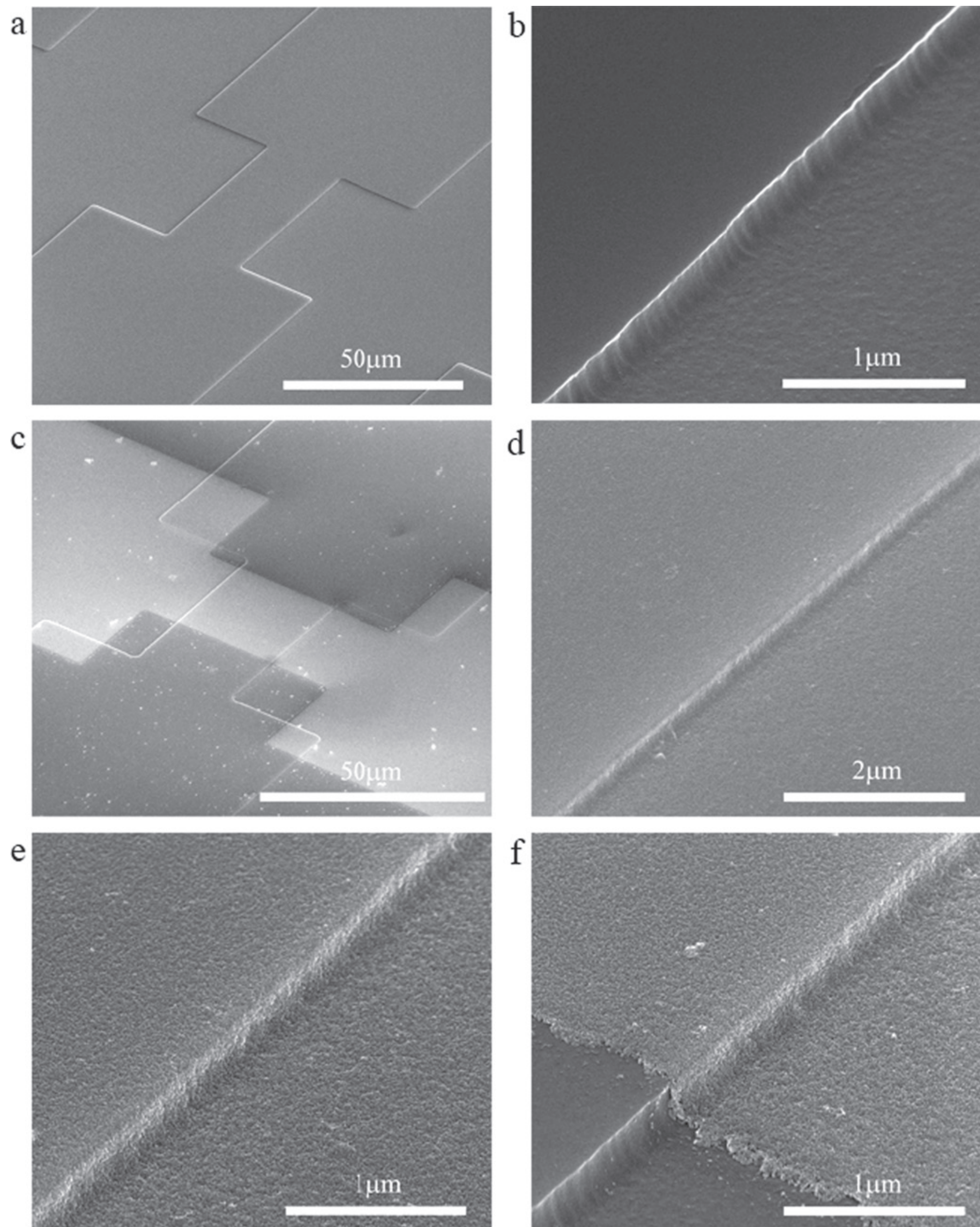

Figure 7. SEM images of 3D silicon substrates (a) and (b) and OH^- terminated PbS QD films on a 220 nm height 3D topography Si substrate (c)–(f).

3.3. Micropatterned QD films—3D substrates

So far, the micropatterning method has been used for pattern formation on flat, 2D substrates. However, to form patterned QD films on more complex integrated circuits that contain, e.g., air clad silicon waveguides or metal electrodes, pattern formation should be extended to substrates with 3D topography. To evaluate the potential of the introduced method for 3D topography micropatterning, we used it on silicon substrates with 3D topography.

To fabricate such substrates, a photoresist was spun on top of a silicon substrate by spin coating and was prebaked to form a robust photoresist layer. After exposure and development, a patterned photoresist layer was formed on top of the silicon substrate. Then reactive-ion etching (RIE) was used to make a 3D structure about 220 nm in height. Afterwards, the photoresist was removed by acetone. The corresponding SEM images of 3D silicon substrates are shown in figures 7(a) and (b). Before the layer-by-layer deposition of the QD film, the 3D substrates were treated with an HF solution (~10%) to enhance the hydrophobicity of the surface and obtain a good wetting of the substrate during the dip-coating (see supporting information V, available at stacks.iop.org/NANO/25/175302/mmedia). The QD films were prepared using six layer-by-layer deposition cycles, and the same wet etching approach was used to pattern the QD films. An HCl/H_3PO_4 mixture in a 1:10 ratio was used for etching, and the same etching times as for the 2D micropatterned QD films were used (see figure 5 and figure S4). The SEM images of micropatterned, OH^- terminated PbS QD films on 3D silicon substrates are shown in

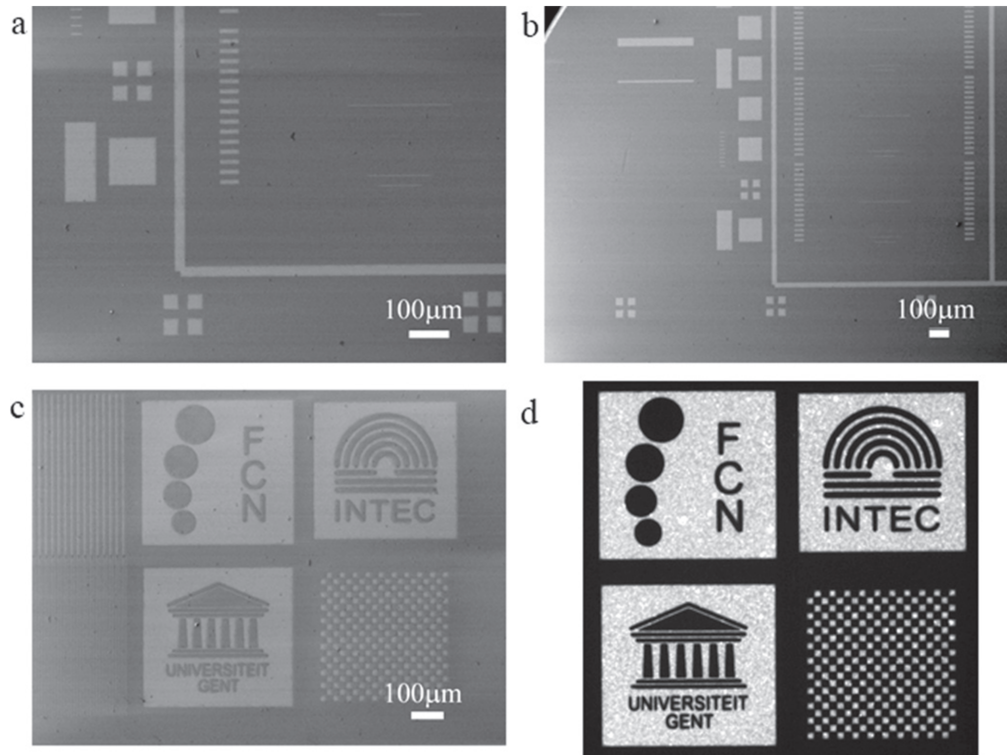

Figure 8. SEM images of a micro-patterned CdSe/CdS QD film on different scales (a)–(c). (d) Fluorescence microscope image of a CdSe/CdS micropatterned film.

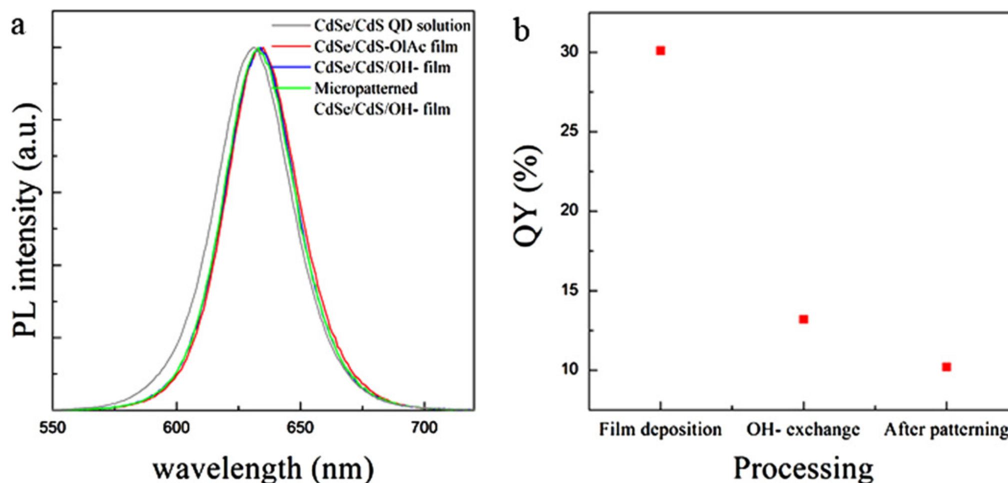

Figure 9. (a) Normalized photoluminescence spectra of CdSe/CdS QD suspension in toluene (grey) and CdSe/CdS QD films terminated with phosphonic acid (red), after OH^- ligand exchange (blue) and after selective wet etching (green). (b) The QY of CdSe/CdS QDs in solution, after deposition, after ligand exchange with OH^- and after micro-patterning with lithography and wet etching.

figures 7(c)–(f). The images show that crack-free and continuous micropatterned PbS QD films were realized on top of the 3D silicon substrates. Similar results have been obtained using S^{2-} terminated PbS QDs (see supporting information IV, figure S5, available at stacks.iop.org/NANO/25/175302/mmedia). We thus conclude that the layer-by-layer deposition and selective wet etching approach can be used to form micropatterned QD films on both 2D and 3D substrates. Clearly, this makes the method highly suitable for the local deposition of films of QDs with inorganic ligands, to be used as active materials in integrated electronic or photonic devices.

3.4. Investigation of the CdSe/CdS QD film

To illustrate the versatility of the patterning recipe, we extended it to CdSe/CdS core/shell QDs by preparing CdSe/CdS QD films under the same conditions as for the PbS films. Also here, TEM analysis evidenced that the original phosphonic acid ligand could be efficiently exchanged for OH^- or S^{2-} moieties (see supporting information VI, available at stacks.iop.org/NANO/25/175302/mmedia). The SEM images shown in figures 8(a)–(c) give an overview of the patterns made, while the fluorescence microscopy image (figure 8(d))

of the same sample gives a first indication that the photoluminescence of the QDs is preserved during the whole process.

A more detailed analysis of the photoluminescence during the different steps of the process showed that the micropatterning hardly affects the emission spectrum of the QDs. As shown in figure 9(a), only a small redshift is found upon film formation, which is not affected by any subsequent treatment. Comparing films of CdSe/CdS QDs with their original ligands, with OH- ligands and after micropatterning, we find that especially the replacement of the phosphonic acid ligands by OH^- (figure 9(b)) leads to a major drop in photoluminescence quantum yield. The micropatterning itself only induces a minor further reduction of the PLQY by about 20%. We thus conclude that the micropatterning—including the wet etching step—leaves the QD's properties largely unaffected.

4. Conclusions

In this paper, we have developed a method for the micropatterning of films of colloidal QDs stabilized by inorganic ligands. Using both PbS and CdSe/CdS QDs, films were made by a layer-by-layer approach, where each cycle involves the deposition of a QD layer by dip-coating, the replacement of the native organic ligands by inorganic moieties, such as OH^- and S^{2-}, followed by a thorough cleaning of the resulting film. We demonstrated that with this method, a smooth and crack-free QD film is formed, on which a photoresist can be spun. The micropatterned films are defined by optical lithography with a positive photoresist, followed by the removal of uncovered QDs by wet etching using a HCl/H_3PO_4 mixture ($1HCl:10H_3PO_4$). High resolution films with feature dimensions down to 500 nm can be realized by this selective wet etching method, limited by the resolution of the lithographic process and a slight over-etching, both on planar and on 3D substrates. For CdSe/CdS core/shell QDs, the micro-patterned films still retained their photoluminescence after lithography and wet etching. Nearly 90% of the QY remains and no additional trap states are introduced in this procedure. These results indicate that the low-cost micropatterning method based on a layer-by-layer approach and selective wet etching is a very promising way to achieve the large-scale device integration of colloidal QDs.

Acknowledgements

This work is supported by Ghent University, the FWO-NanoMIR project, the FP7-ERC-MIRACLE project and the IAP photonics@be network. We acknowledge the assistance from Steven Verstuyft during the device fabrication. We also acknowledge the assistance from Liesbet Van Landschoot and Kasia Komorowska during SEM measurements, and Katrien Haustraete during TEM measurements.

References

[1] Liu H, Zhitomirsky D, Hoogland S, Tang J, Kramer I J, Ning Z and Sargent E H 2012 *Appl. Phys. Lett.* **101** 151112
[2] Arango A C, Oertel D C, Xu Y, Bawendi M G and Bulovic V 2009 *Nano Lett.* **9** 860
[3] Ma W, Swisher S L, Ewers T, Engel J, Ferry V E, Atwater H A and Alivisatos A P 2011 *ACS Nano* **5** 8140
[4] Keuleyan S, Lhuillier E, Brajuskovic V and Guyot-Sionnest P 2011 *Nature Photonics* **5** 489
[5] Clifford J P, Konstantatos G, Johnston K W, Hoogland S, Levina L and Sargent E H 2008 *Nature Nanotechnology* **4** 40
[6] Rauch T, Boberl M, Tedde S F, Furst J, Kovalenko M V, Hesser G N, Lemmer U, Heiss W and Hayden O 2009 *Nature Photonics* **3** 332
[7] Dang C, Lee J, Zhang Y, Han J, Breen C, Steckel J S, Coe-Sullivan S and Nurmikko A 2012 *Adv. Mater.* **24** 5915
[8] Pal B N, Ghosh Y, Brovelli S, Laocharoensuk R, Klimov V I, Hollingsworth J A and Htoon H 2012 *Nano Lett.* **12** 331
[9] Moreels I, Justo Y, Geyter B D, Haustraete K, Martins J C and Hens Z 2011 *ACS Nano* **5** 2004
[10] Kovalenko M V, Kaufmann E, Pachinger D, Roither J, Huber M, Stangl J, Hesser G, Schaffler F and Heiss W 2006 *J. Am. Chem. Soc.* **128** 3516
[11] Moreels I *et al* 2009 *ACS Nano* **3** 3023
[12] Coe-Sullivan S, Steckel J S, Woo W-K, Bawendi M G and Bulovic V 2005 *Advanced Functional Materials* **15** 1117
[13] Singh M, Haverinen H M, Dhagat P and Jabbour G E 2010 *Adv. Mater.* **22** 673
[14] Böberl M, Kovalenko M V, Gamerith S, List E J W and Heiss W 2007 *Adv. Mater.* **19** 3574
[15] Tekin E, Smith P J, Hoeppener S, Van den Berg A M J, Susha A S, Rogach A L, Feldmann J and Schubert U S 2007 *Advanced Functional Materials* **17** 23
[16] Urban J J, Talapin D V, Shevchenko E V and Murray C B 2006 *J. Am. Chem. Soc.* **128** 3248
[17] Justo Y, Moreels I, Lambert K and Hens Z 2010 *Nanotechnology* **21** 295606
[18] Lambert K, Capek R K, Bodnarchuk M I, Kovalenko M V, Van Thourhout D, Heiss W and Hens Z 2010 *Langmuir* **26** 7732
[19] Bourvon H, Calvez S L, Kanaan H, Meunier-Della-Gatta S, Philippot C and Reiss P 2012 *Adv. Mater.* **24** 4414
[20] Tang J *et al* 2011 *Nature Materials* **10** 765
[21] Ning Z *et al* 2013 *Adv. Mater.* **25** 1719
[22] Konstantatos G and Sargent E H 2010 *Nature Nanotechnology* **5** 391
[23] Chen M, Yu H, Kershaw S V, Xu H, Gupta S, Hetsch F, Rogach A L and Zhao N 2013 *Advanced Functional Materials* **24** 53
[24] Choi J-H, Fafarman A T, Oh S J, Ko D-K, Kim D K, Diroll B T, Muramoto S, Gillen J G, Murray C B and Kagan C R 2012 *Nano Lett.* **12** 2631
[25] Talapin D V, Lee J-S, Kovalenko M V and Shevchenko E V 2010 *Chemical Reviews* **110** 389
[26] Ip A H *et al* 2012 *Nature Nanotechnology* **7** 577–82
[27] Konstantatos G, Badioli M, Gaudreau L, Osmond J, Bernechea M, Arquer F P G, Gatti F and Koppens F H L 2012 *Nature Nanotechnology* **7** 363–8
[28] Talgorn E, Vries M A, Siebbeles L D A and Houtepen A J 2011 *ACS Nano* **5** 3552
[29] Bae W K, Kwak J, Lim J, Lee D, Nam M K, Char K, Lee C and Lee S 2010 *Nano Lett.* **10** 2368
[30] Semonin O E, Luther J M, Choi S, Chen H-Y, Gao J, Nozik A J and Beard M C 2011 *Science* **334** 1530–3
[31] Liu W, Lee J-S and Talapin D V 2013 *J. Am. Chem. Soc.* **135** 1349

[32] Lambert K, Moreels I, Van Thourhout D and Hens Z 2008 *Langmuir* **24** 5961
[33] Park Y *et al* 2012 *Nanotechnology* **23** 355302
[34] Nandwana V, Subramani C, Yeh Y-C, Yang B, Dickert S, D Barnes M, T Tuominenb M and M Rotello V 2011 *Journal of Materials Chemistry* **21** 16859
[35] Kim L A, Anikeeva P O, Coe-Sullivan S A, Steckel J S, Bawendi M G and Bulovic V 2008 *Nano Lett.* **8** 4513
[36] J Gassensmith J, M Erne P, F Paxton W, Frasconi M, D Donakowski M and Stoddart J F 2013 *Adv. Mater.* **25** 223
[37] Kramer R K, Pholchai N, Sorger V J, Yim T J, Oulton R and Zhang X 2010 *Nanotechnology* **21** 145307
[38] Lalander C H, Zheng Y, Dhuey S, Cabrini S and Bach U 2010 *ACS Nano* **4** 6153
[39] Nag A, Kovalenko M V, Lee J-S, Liu W, Spokoyny B and Talapin D V 2011 *J. Am. Chem. Soc.* **133** 10612
[40] Cademartiri L, Montanari E, Calestani G, Migliori A, Guagliardi A and Ozin G 2006 *J. Am. Chem. Soc.* **128** 10337
[41] Carbone L, Nobile C, Giorgi M D, Sala F D, Morello G *et al* 2007 *Nano Lett.* **7** 2942–50
[42] Hu C, Gassenq A, Justo Y, Yakunin S, Heiss W, Hens Z and Roelkens G 2013 *Proc. of Int. Conf. SPIE 8631 Quantum Sensing and Nanophotonic Devices X* (*San Francisco, US 2-7 February 2013)*
[43] Montalti M, Credi A, Luca P and Gandolfi T M 2006 *Handbook of Photochemistry* 3rd edn (Boca Raton, FL: CRC Press)